Supporting Information

Cholesterol-Based Diazine Derivative: Selective Sensing of Ag^+ and Fe^{3+} Ions through Gelation and the Performance of Metallogels in Dye and Picric Acid Adsorption from water

Atanu Panja and Kumaresh Ghosh*

Department of Chemistry, University of Kalyani, Kalyani-741235, India.
Email: ghosh_k2003@yahoo.co.in; kumareshchem18@klyuniv.ac.in

Table 1S. Results of gelation test for compound **1**.

Solvent	1
DMSO	PS
DMF	PS
CH_3CN	PS
THF	S
CH_3OH	I
Toluene	**G**
$CHCl_3$	S
Cyclohexane	S
DMSO : H_2O(1:1,v/v)	I
DMF : H_2O (1:1,v/v)	I
CH_3CN : H_2O (1:1,v/v)	I
THF: H_2O (1:1,v/v)	S
CH_3OH : H_2O (1:1,v/v)	I
$CHCl_3$: CH_3OH (1:1, v/v)	P
$CHCl_3$: CH_3OH (1:2, v/v)	P
$CHCl_3$: CH_3OH (3:1, v/v)	S
Toluene : CH_3OH (1:1, v/v)	S
Ethanol : H_2O (1:1,v/v)	I
THF : H_2O(1:1,v/v) + Cu^{2+}	P
THF : H_2O(1:1,v/v) + Hg^{2+}	P
THF : H_2O(1:1,v/v) + Ag^+	P
$CHCl_3$: CH_3OH (3:1, v/v) + Ag^+	**G**
$CHCl_3$: CH_3OH (3:1, v/v) + Fe^{3+}	**G**
S = solution; G = gel; PS = partially soluble; PG = partial gel; I = insoluble; P = Precipitation.	

Fig. 1S. Pictorial representation of the effect of Ag^+ and Fe^{3+} ions on phase changes of **3** in $CHCl_3/CH_3OH$ (3:1, v/v). None of the said metal ions caused gelation of **3** under experimental conditions.

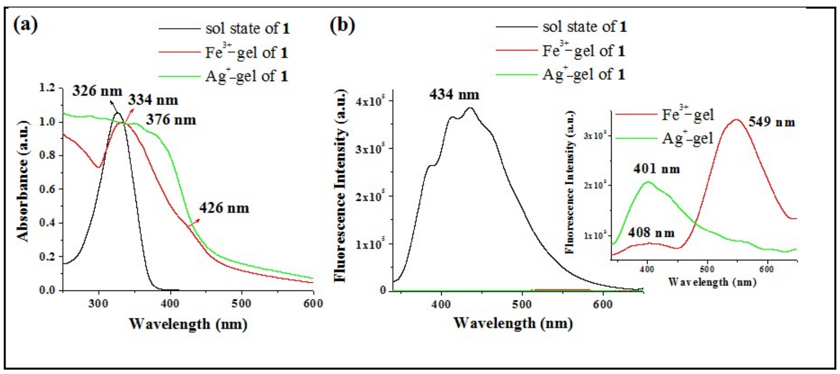

Fig. 2S. Comparison of (a) normalized UV–vis and (b) fluorescence spectra (λ_{ex} = 330 nm) of **1** in the sol and gel states. Inset of (b) signifies the expanded version.

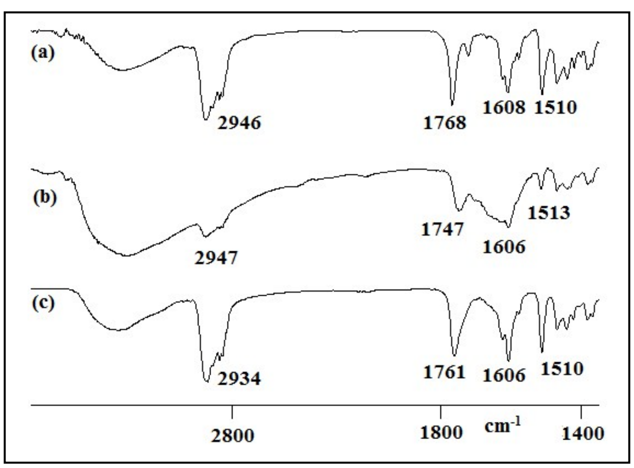

Fig. 3S. Partial FTIR spectra of **1** in (a) amorphous state and gel state with (b) $Fe^{3+}$and (c) Ag^+ ions.

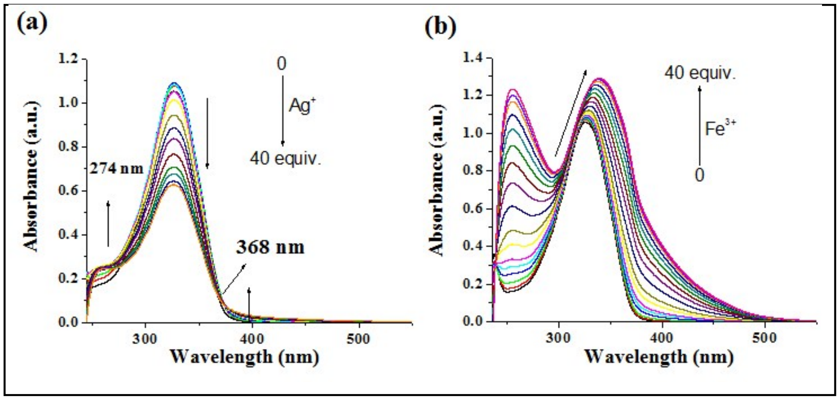

Fig. 4S. Change in absorbance of **1** (c = 2.50 x 10^{-5} M) upon addition of 40 equiv. amounts (a) Fe^{3+} and (b) Ag^{+} ions (c = 1.0 x 10^{-3} M) in $CHCl_3/CH_3OH$ (3:1, v/v).

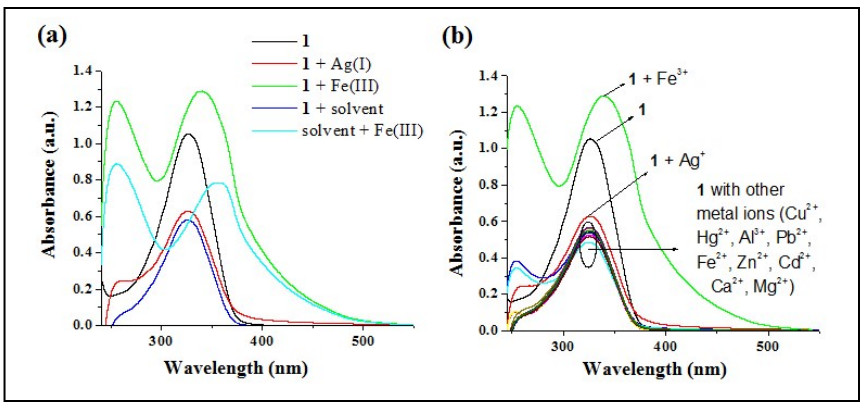

Fig. 5S. Comparative plots of absorption changes of **1** (c = 2.50 x 10^{-5} M) with (a) solvent and (b) different metal ions (40 equiv., c = 1.0 x 10^{-3} M) in $CHCl_3/CH_3OH$ (3:1, v/v).

.

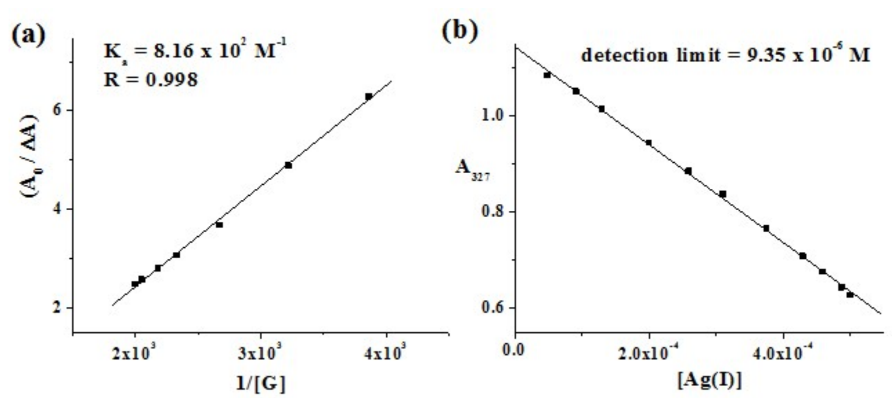

Fig. 6S. (a) Benesi–Hilderband plot and (b) detection limit for **1** (c = 2.5 x 10^{-5} M) with Ag^{+} ion (c = 1.0 x 10^{-3} M) at 327 nm in $CHCl_3/CH_3OH$ (3:1, v/v) from UV-vis titration.

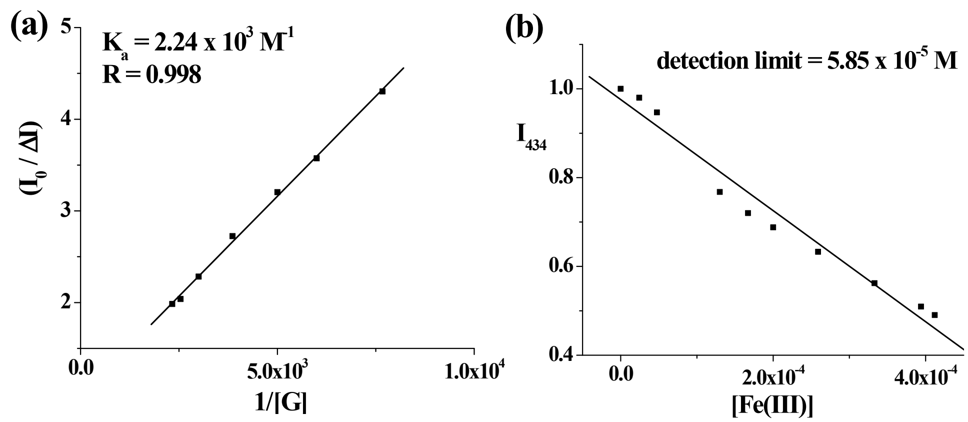

Fig. 7S. (a) Benesi–Hilderband plot and (b) detection limit for **1** (c = 2.5 x 10^{-5} M) with Fe^{3+} ion (c = 1.0 x 10^{-3} M) at 434 nm in $CHCl_3/CH_3OH$ (3:1, v/v) from fluorescence titration.

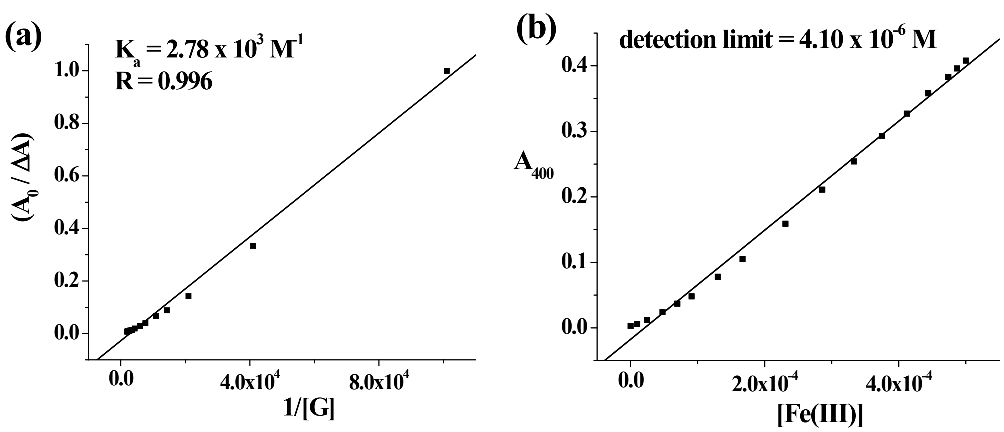

Fig. 8S. (a) Benesi–Hilderband plot and (b) detection limit for **1** (c = 2.5 x 10^{-5} M) with Fe^{3+} ion (c = 1.0 x 10^{-3} M) at 400 nm in $CHCl_3/CH_3OH$ (3:1, v/v) from UV-vis titration.

Table 2S. Binding constant and detection limit values of the metal-**1** complexes.

Metal-ligand complex	Binding constant values (M^{-1})	
	From UV-vis titration	From fluorescence titration
1 – Ag^{+}	K = 8.16 x 10^{2}	-
1 – Fe^{3+}	K = 2.78 x 10^{3}	K = 2.24 x 10^{3}

Metal-ligand complex	Detection limit values (M)	
	From UV-vis titration	From fluorescence titration
1 – Ag^{+}	9.35 x 10^{-6}	-
1 – Fe^{3+}	4.10 x 10^{-6}	5.85 x 10^{-5}

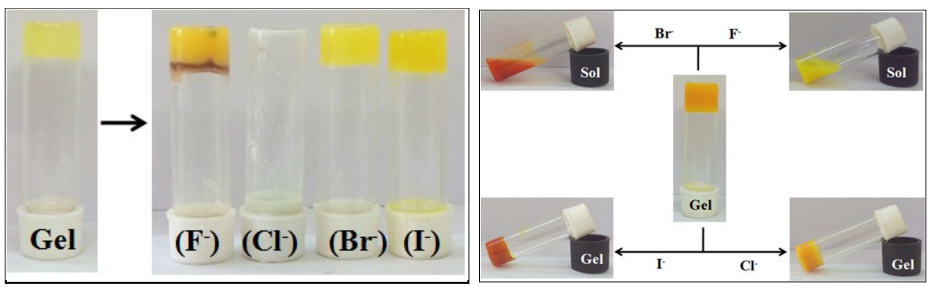

Fig. 9S. Photograph showing the chemical responsiveness of the Ag^{+}-induced (left) and Fe^{3+}-induced (right) gel of **1** toward different halides.

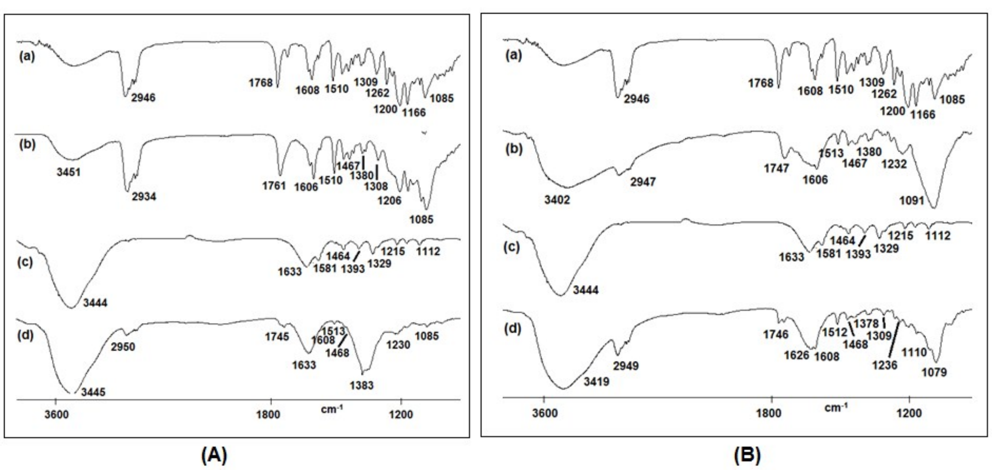

Fig. 10S. (A) Partial FTIR spectra of (a) **1**, (b) **1**-Fe^{3+} gel, (c) Uranine and (d) Uranine adsorbed **1**-Fe^{3+} gel. (B) Partial FTIR spectra of (a) **1**, (b) **1**-Ag^{+} gel, (c) Uranine and (d) Uranine adsorbed **1**-Ag^{+} gel.

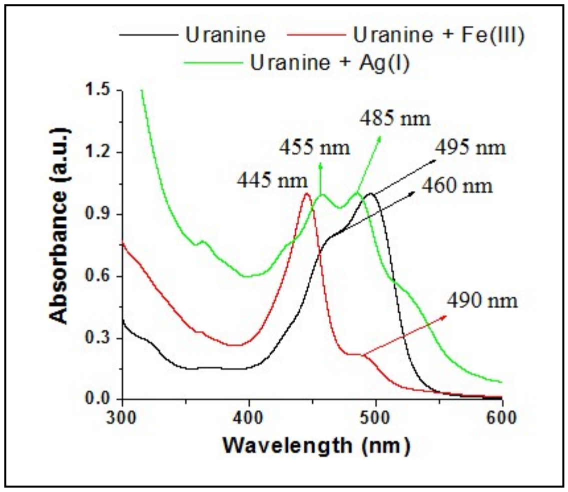

Fig. 11S. Comparision of normalized UV-vis spectra of Uranine in absence and presence of Fe^{3+} and Ag^{+} ions in $CHCl_3/CH_3OH$ (3:1, v/v) containing 1% H_2O.

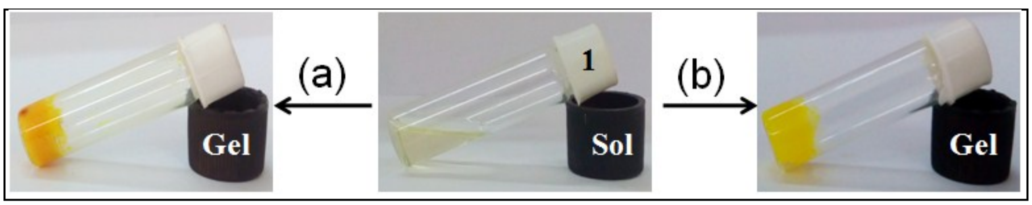

Fig. 12S. Photograph representing the gel formation of **1** in $CHCl_3/CH_3OH$ (3:1, v/v) upon simultaneous addition of (a) Fe^{3+} and PA and (b) Ag^{+} and PA.

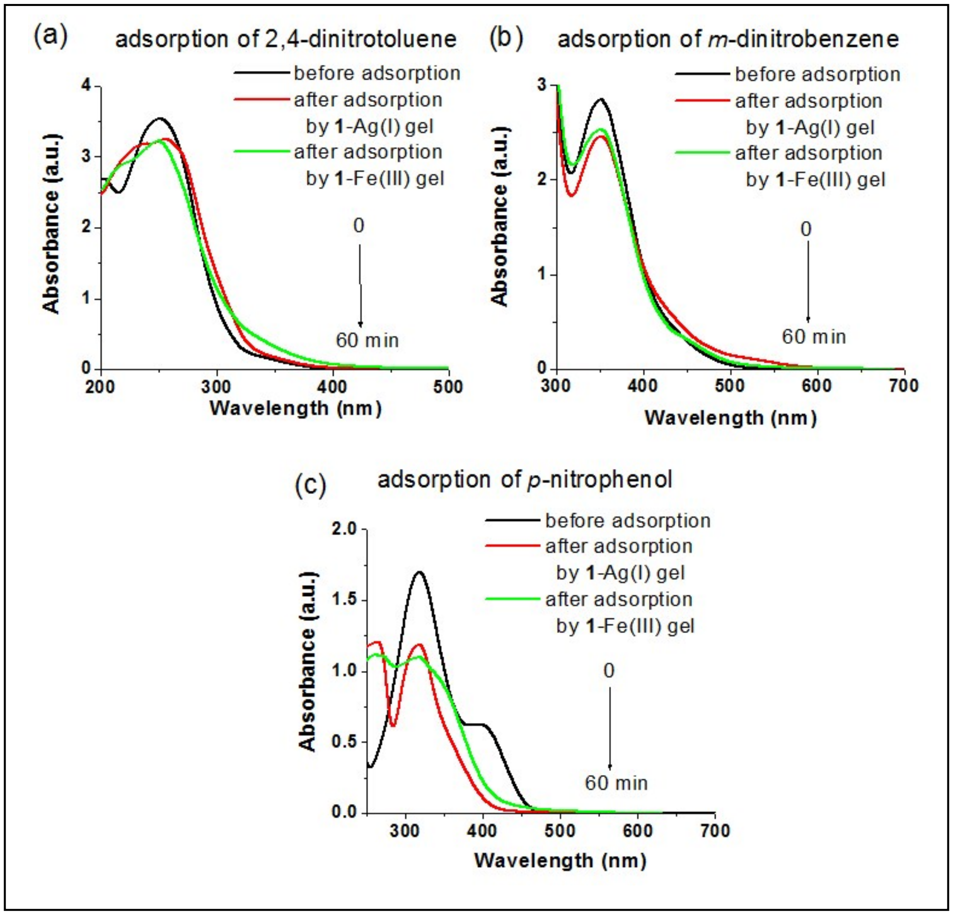

Fig. 13S. Change in absorbance of (a) 2,4-dinitrotoluene, (b) *m*-dinitrobenzene and (c) *p*-nitrophenol during adsorption by **1**-Fe^{3+} and (b) **1**-Ag^{+} gels [For *m*-dinitrobenzene, $c = 1 \times 10^{-4}$ M; for other cases, $c = 2 \times 10^{-4}$ M; for all the compounds, 3 mL of aqueous solution containing 0.01% CH_3CN was used for the experiment. The gels were initially prepared by adding equiv. amount of respective metal salts to **1** (25 mg/mL) in $CHCl_3/CH_3OH$ (3:1, v/v)].

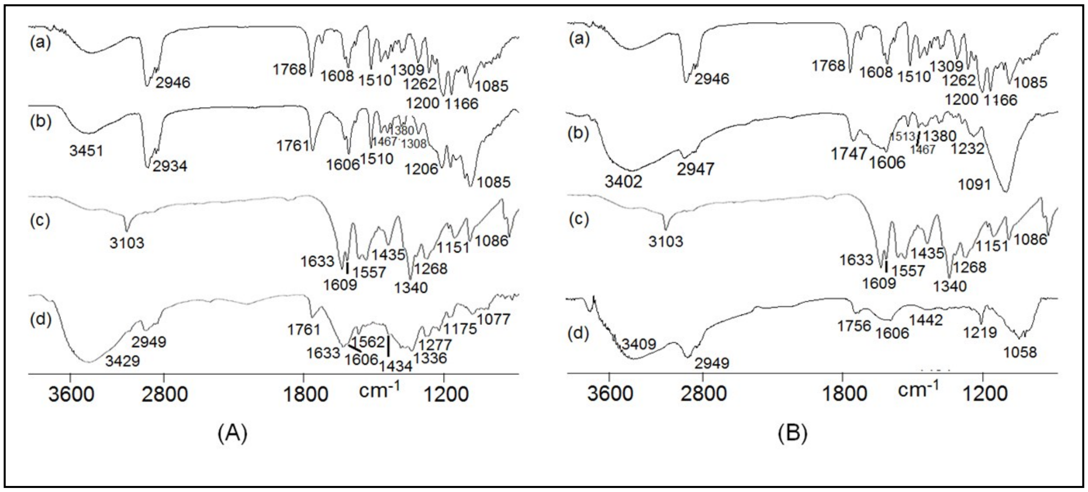

Fig. 10S. (A) Partial FTIR spectra of (a) **1**, (b) **1**-Ag^{+} gel, (c) PA and (d) PA adsorbed **1**-Ag^{+} gel. (B) Partial FTIR spectra of (a) **1**, (b) **1**-Fe^{3+} gel, (c) PA and (d) PA adsorbed **1**-Fe^{3+} gel.

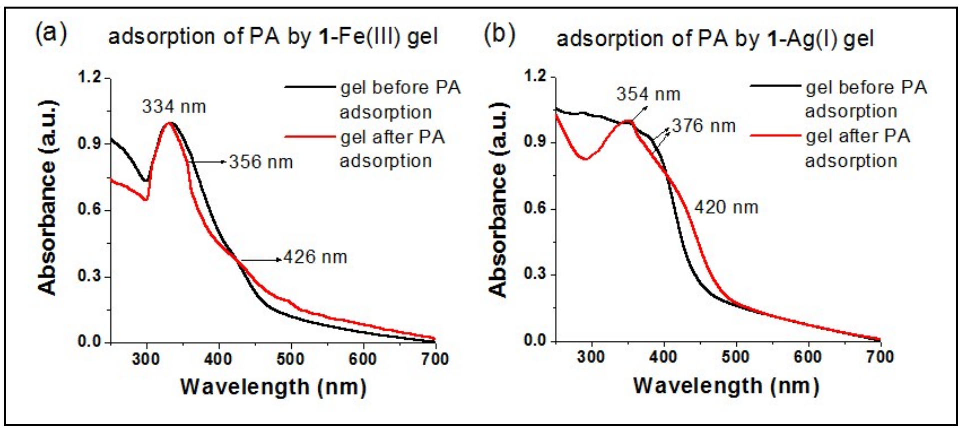

Fig. 15S. Comparison of normalized UV–vis spectra of (a) **1**-Fe^{3+} gel and (b) **1**-Ag^{+} gel, before and after adsorption of PA.

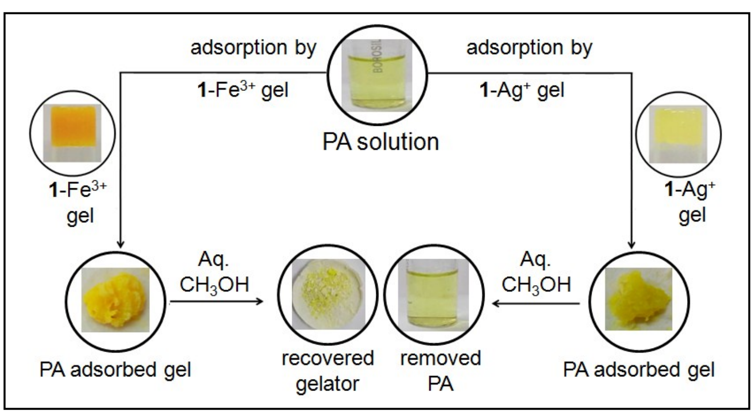

Fig. 16S. Photograph showing the recyclability of the PA adsorption process.

Table 3S. Reported structures for Fe^{3+} sensing in solution and gel phase

Entry	Gelator structure	Gelation	Sensing mechanism	solvent	Interference from other metal ions	Ref.
1	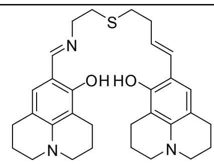	No gelation	Colorimetric sensing	MeOH–buffer solution (9 : 1, v/v, 10 mM, bis-tris, pH 7.0)	Fe^{2+}	1c
2	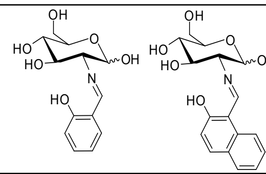	No gelation	Colorimetric sensing	MeOH aqueous HEPES buffer at pH 7.2	Fe^{2+}, Cu^{2+} Fe^{2+}, Cu^{2+}	1d
3	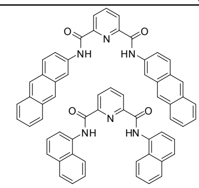	No gelation	Fluorescence OFF	THF	Fe^{2+}	1e
4	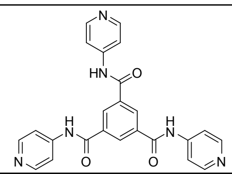	**Gelation**	Sol to gel transition	Water	Fe^{2+}	1a
5	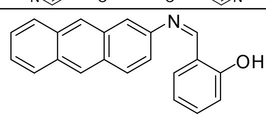	No gelation	Fluorescence ON	THF	Fe^{2+}	1f
6	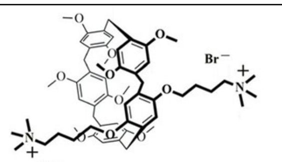	**Gelation**	Fluorescence OFF Gel-to-Gel state	H_2O	-	1b
7	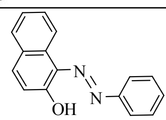	**Gelation**	Visual detection through gel-to-sol transition	CH_3CN/ H_2O (1:1)	Cu^{2+}	1g
8	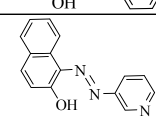	**Gelation**	Visual detection through gel-to-sol transition	CH_3CN/ H_2O (1:1)	-	1g
9	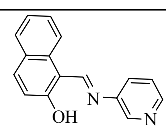	**Gelation**	Visual detection through color change	DMSO/ H_2O (1:1)	-	1g
This work	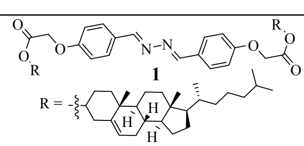	**Gelation**	Visual detection through sol-to-gel transition	$CHCl_3/CH_3OH$ (3:1, v/v)	Ag^+ (No interference from Fe^{2+})	-

Table 4S. Adsorption of Picric acid (PA) by different adsorbents

Entry	Adsorbent	Removal efficiency for PA (%)	Ref.
1	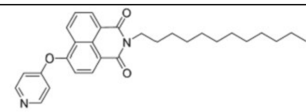 Low molecular weight gelator (LMWG)	**56.86** (from absorption spectroscopic study)	2a
2	carbon nanotubes	83.2	2b
3	active carbon	>99	2c
4	Amberlite IRA-67	96	2d
5	Mesoporous MCM-41	>82	2e
6	iron oxide nanoparticles	99	2f
This work	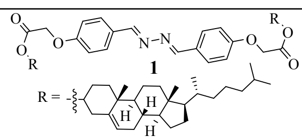 Low molecular weight gelator (LMWG)	**83**% (by **1**-Fe^{3+} gel) **74**% (by **1**-Ag^{+} gel)	-

1. (a) J. –L. Zhong, X. –J. Jia, H. –J. Liu, X. –Z. Luo,S. –G. Hong, N. Zhanga and J. –B. Huang, *SoftMatter*, 2016, **12**, 191; (b) J. –F. Chen, Q. Lin, H. Yao, Y. –M. Zhang and T. –B. Wei, *Mater. Chem. Front.*, 2018, **2**, 999; (c) Y. S. Kim, G. J. Park, J. J. Lee, S. Y. Lee, S. Y. Lee and C. Kim, *RSC Adv.*, 2015, **5**, 11229; (d) A. Mitra, B. Ramanujam and C. P. Rao, *Tetrahedron Lett.*, 2009, **50**, 776; (e) P. Kumar, V. Kumar and R. Gupta, *RSC Adv.*, 2015, **5**, 97874; (f) S. Sen, S. Sarkar, B. Chattopadhyay, A. Moirangthem, A. Basu, K. Dhara and P. Chattopadhyay, *Analyst*, 2012, **137**, 3335; (g) A. Panja and K. Ghosh, *Mater. Chem. Front.,* 2018, DOI: 10.1039/c8qm00257f.

2. (a) X. Cao, N. Zhao, H. Lv, Q. Ding, A. Gao, Q. Jing and T. Yi, *Langmuir*, 2017, **33**, 7788; (b) S. Gholitabar and H. Tahermansouri, *Carbon Lett.*, 2017, **22**, 14; (c) R. Qadeer and A. H. Rehan, *Turk. J. Chem.*, 2002, 26, 557; (d) H. Uslu, and G. Demir, *J. Chem. Eng. Data*, 2010**, 55***,* 3290; (e) H. Sepehrian, J. Fasihi and M. K. Mahani, *Ind. Eng. Chem. Res.*, 2009**, 48***,* 6772; (f) H. Parham, B. Zargar and M. Rezazadeh, *Mater. Sci. Eng. C.*, 2012, **32**, 2109.

^{1}H NMR ($CDCl_3$, 400 MHz)

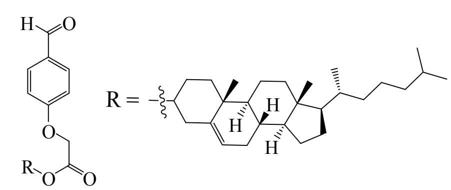

3

^{13}C NMR ($CDCl_3$, 100 MHz)

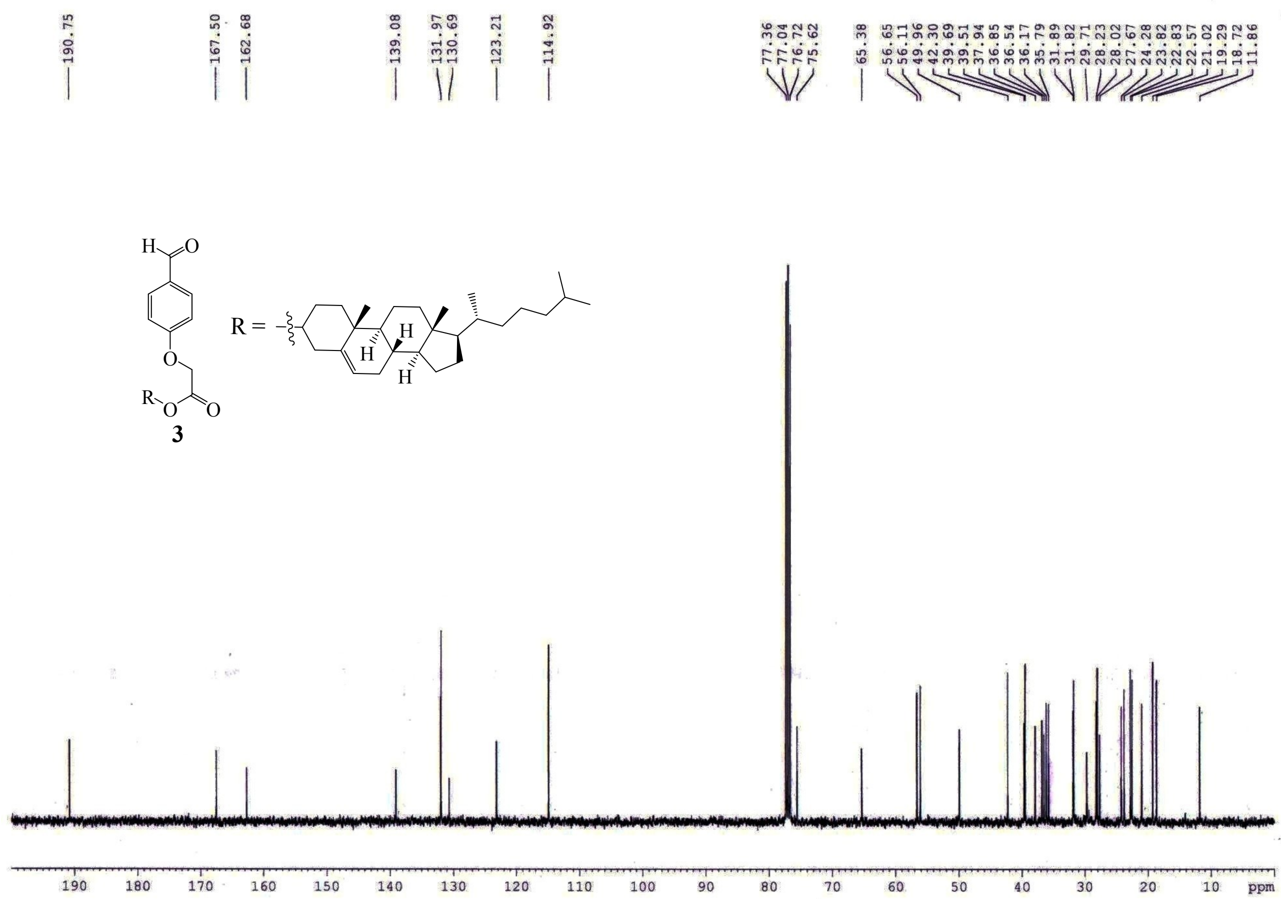

Mass spectrum of 3.

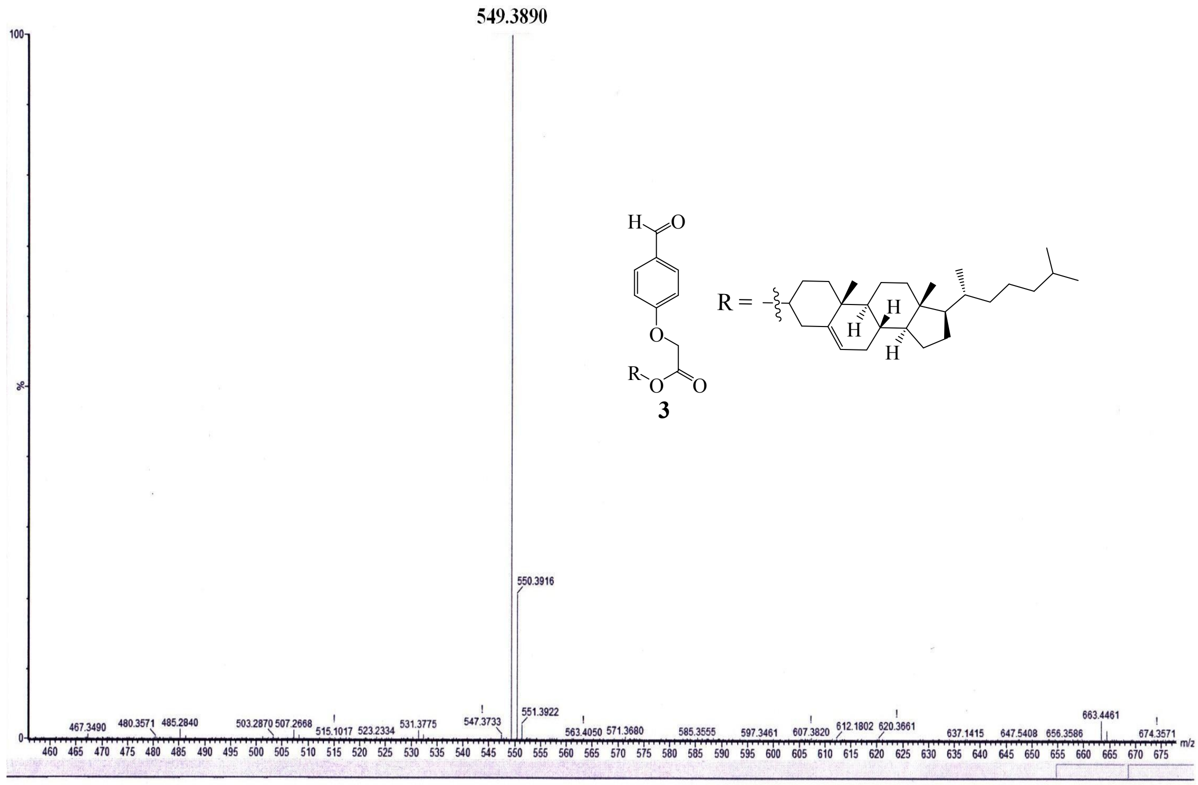

^{1}H NMR ($CDCl_3$, 400 MHz)

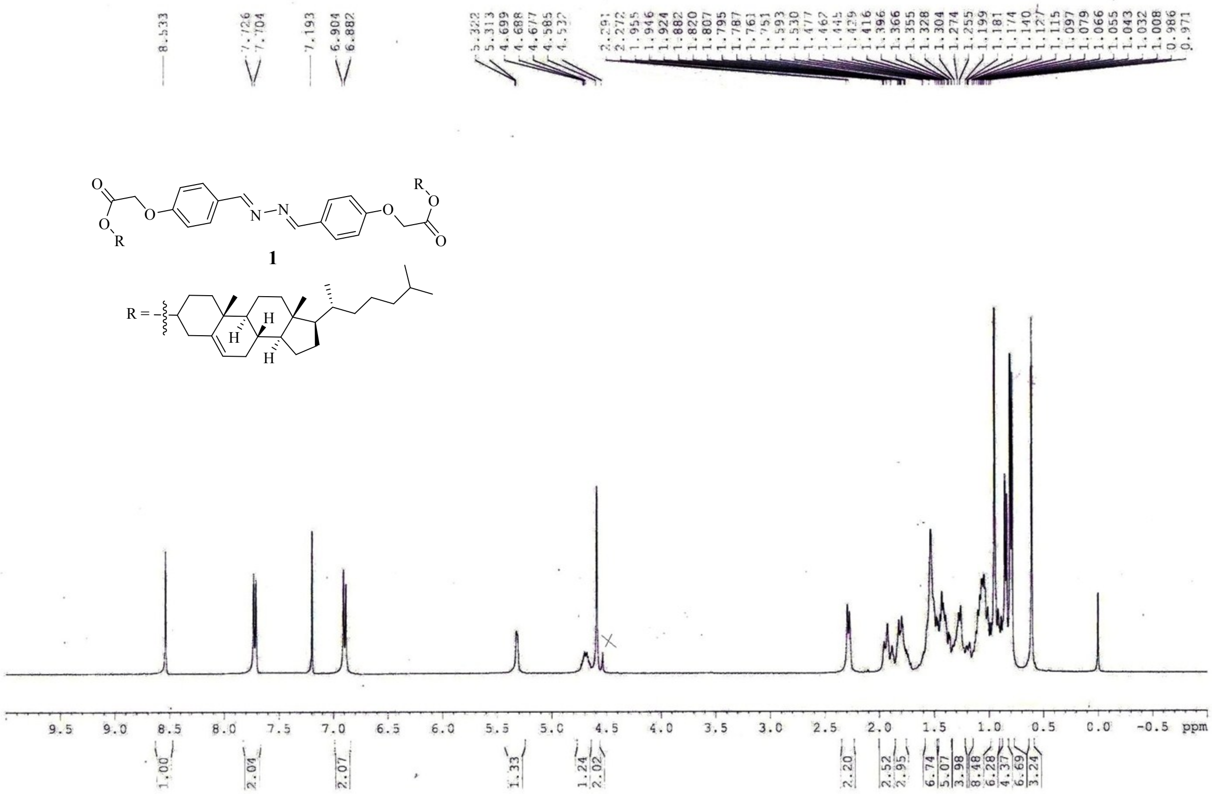

^{13}C NMR (CDCl$_3$, 100 MHz)

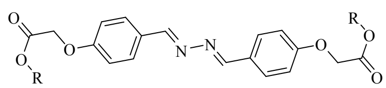
1

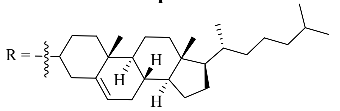
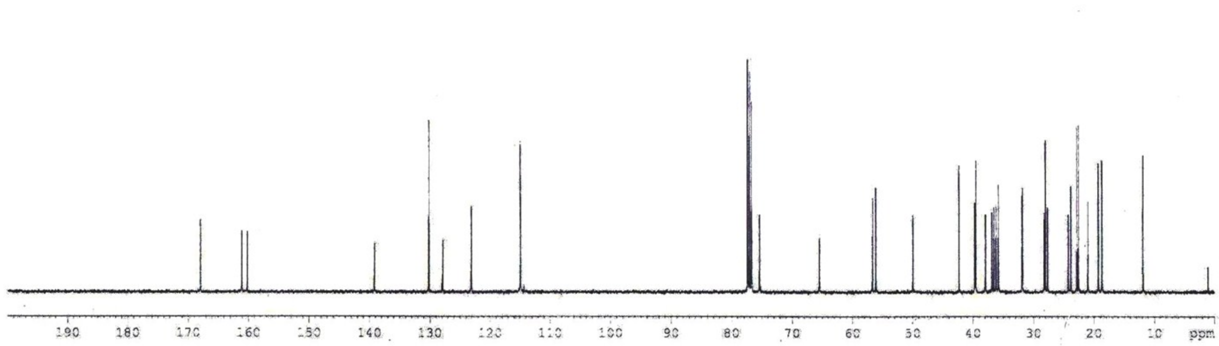

Mass spectrum of 1.